arXiv:2008.02506v1 [quant-ph] 6 Aug 2020

Scattering of Spin-$\frac{1}{2}$ Particles from a $\mathcal{PT}$-symmetric Complex Potential

Ege Özgün,[1,*] T. Hakioğlu,[2,3] and Ekmel Ozbay[1,4]

[1] *NANOTAM-Nanotechnology Research Center, Bilkent University, 06800 Ankara, Turkey*
[2] *Energy Institute and Department of Physics,İstanbul Technical University,34469 İstanbul, Turkey*
[3] *Department of Physics, Northeastern University, Boston, MA 02115 , USA*
[4] *Department of Physics, Department of Electrical and Electronics Engineering and UNAM-Institute of Materials Science and Nanotechnology, Bilkent University, 06800 Ankara, Turkey*

In this letter, we study the scattering of spin-$\frac{1}{2}$ particles from a spin-independent parity time ($\mathcal{PT}$)-symmetric complex potential, and for the first time, theoretically demonstrate the coexistence of $\mathcal{PT}$-symmetric and $\mathcal{PT}$-broken phases for broadband energy spectra in this system. We also show the existence of anisotropic transmission resonances, accessible through the tuning of energy. Our results are promising for applications in spintronics, semiconductor-based devices, and a better understanding of the topological surface states.

I. INTRODUCTION

With their gamechanger paper published in 1998 [1], Bender and Boettcher questioned the condition of Hermiticity as a seventy-year-old conceptual foundation in quantum mechanics and proposed that [1, 2] it should be replaced by the $\mathcal{PT}$-symmetry. In a series of three manuscripts [4], Mostafazadeh introduced the concept of pseudo-Hermiticity and showed that every Hamiltonian with real spectra is pseudo-Hermitian and that the $\mathcal{PT}$-symmetric Hamiltonians all belong to that class of pseudo-Hermitian Hamiltonians. Later, in the light of $\mathcal{PT}$-symmetric quantum mechanics, thanks to the analogy between Schrödinger's equation and the equation for the propagation of an electromagnetic wave under paraxial approximation, $\mathcal{PT}$-symmetry studies were ignited in the field of classical optics [5–12]. The studies on optical systems with equal loss/gain media that show $\mathcal{PT}$-symmetric nature, gave rise to the derivation of generalized unitarity relation [13], also coined as the pseudo-unitarity condition, which was studied later on within the context of quantum mechanical scattering [14, 15]. Although there is an ocean of significant theoretical studies on $\mathcal{PT}$-symmetric structures, the experimental proposals and demonstrations are far more limited. Observation of $\mathcal{PT}$-symmetry breaking in optical systems [9, 11], $\mathcal{PT}$-symmetry in optically induced atomic lattices [16], in a single quantum system [17], with superconducting quantum circuits [18], experimental realization of Floquet $\mathcal{PT}$-symmetric systems [19], demonstration of optical anti-$\mathcal{PT}$-symmetry in a warm atomic-vapour cell [20], applications of $\mathcal{PT}$-symmetry in optics including proposals and demonsrations of lasing [21], cloaking [22, 23] and uni-directional invisibility [24], and proposals for experimental realizations within the context of condensed matter physics [25] and atomic gases [26] are among those. There are also reviews [27–29] and books [30, 31] covering all of the details of the subject that are excluded within the scope of this letter.

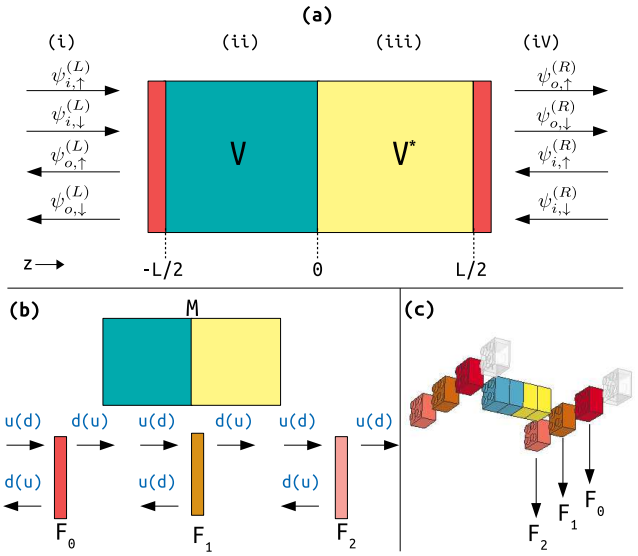


FIG. 1. **(a)** Overview of the structure **(b)** The abilities of symmetric (F_0) and asymmetric (F_1 and F_2) spin flippers (SF), (F=L/R for left/right). u(d) denotes up(down) spin states. **(c)** The schematic of 16 possible configurations, where the transparent component means not using any SF.

Recently, a photonic heterostructure with one-dimensional gain/loss bilayer and polarization converting components, which allowed $\mathcal{PT}$-symmetric and $\mathcal{PT}$-broken eigenvalues to coexist simultaneously for broadband wavelengths, was studied [32]. In this paper, through a simple yet intuitive problem of one-dimensional scattering of spin-$\frac{1}{2}$ particles from a spin-independent, complex, non-Hermitian $\mathcal{PT}$-symmetric potential, we study the quantum mechanical analog of that photonic problem and theoretically demonstrate the mixing of $\mathcal{PT}$-symmetric and $\mathcal{PT}$-broken eigenvalues of the scattering ($\mathbb{S}$) matrix. To the best of our knowledge this problem has also not been studied in the context of quantum device applications. The possibility of obtaining mixed phase is already giving rise to intriguing research in the field of photonics [**?**], which makes our

* ozgune@bilkent.edu.tr

results even more important, since we are expecting the onset of similar research in the field of quantum mechanics.

II. PROPOSED STRUCTURE AND THEORY

Our system, as given in Fig. 1, consists of a $\mathcal{PT}$-symmetric complex potential region (M), with $V = V_R + iV_I$, $[V_R, V_I \in \Re]$ satisfying the $\mathcal{PT}$-symmetry condition $V(z) = V^*(-z)$ and three different types of spin flippers (SF), that create a four-channel system -two input and two output channels for up (u) and down (d) spins that can be attached to both ends of M. Various proposals for such $\mathcal{PT}$-symmetric structures are given in the introduction part of this manuscript and is not our main focus. Incoming and outgoing wavefunctions of the spin-$\frac{1}{2}$ particles are shown in Fig. 1(a). The SFs flip the spin of the reflected and transmitted spin-$\frac{1}{2}$ particles in the following way as shown in Fig. 1(b): The symmetric SF F_0 flips the spin of both reflected and transmitted spin-$\frac{1}{2}$ particles from u(d) to d(u), whereas the asymmetric SF F_1 only flips the spin of the transmitted ones and F_2 does the opposite and only flips the spin of the reflected ones. The SFs are heterojunction interfaces based on materials with strong spin-dependent potentials operating on a certain incoming spin state $|S_i\rangle = a|\uparrow\rangle + b|\downarrow\rangle$. Their basic function is to manipulate the Bloch-sphere of the transmitted $|S_t\rangle$ and the reflected $|S_r\rangle$ states by external parameters like the electric field vector $\mathbf{E}$ and the controllable gates that can be tuned externally [33]. Moreover, it was theoretically demonstrated that it is possible to obtain strongly spin-flipping resonances, which are required for the SFs proposed in this letter, in quantum well structures by exploting the Rashba and Dresselhaus spin orbit couplings [34]. III-V group semiconductor heterostructure quantum wells with sizes $(10 - 70\ nm)$ proposed in Ref. [34] can be fabricated using conventional epitaxial techniques, such as Molecular Beam Epitaxy, Atomic Layer Deposition, and Metalorganic Chemical Vapour Deposition [35]. Here, we assume that the SFs only manipulate the spin degree of freedom of the incoming spin-$\frac{1}{2}$ particles and not the overall reflection-transmission profile, which provides a simplification in calculations. We can safely do this, since our main results, that are mixing of $\mathcal{PT}$-symmetric and $\mathcal{PT}$-broken phases and the existence of anisotropic transmission resonances (ATR), would still be valid without the assumption.

We relabel the SFs (F) as R and L for right and left placement, so that we have three different possibilities for right placement R_0, R_1, R_2, and three for left placement L_0, L_1, L_2. Also taking into account that we can choose to not use any of those for right and left and only stick with M (illustrated with the transparent component), we have 16 different possibilities in total, summarized in the schematic given in Fig. 1(c). Let us first lay the physics of the problem before investigating these possible

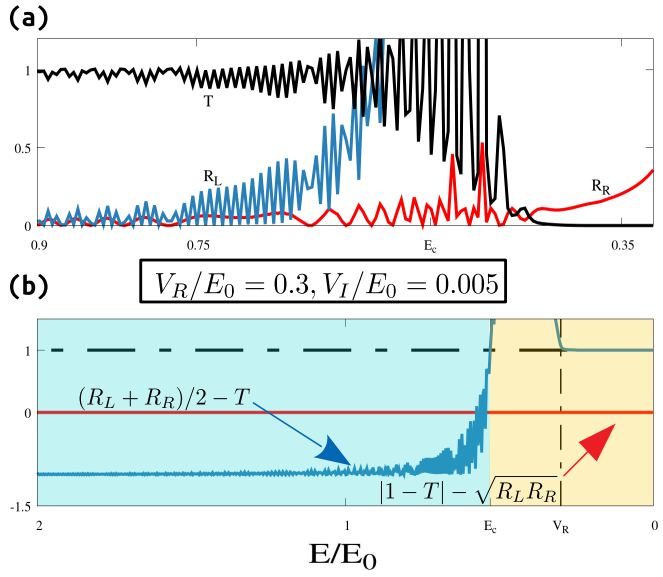


FIG. 2. **(a)** For $L = 0.5\ \mu m$, $V_R/E_0 = 0.3, V_I/E_0 = 0.005$, R_L (blue), R_R (red) and T (black) are plotted versus dimensionless energy E/E_0, where $E_0 = 1\ eV$. The anisotropic transmission resonances (ATR), are shown, where both $R_R = 0$, $T = 1$ and $R_L = 0$, $T = 1$ are obtained for varying energies. **(b)** The pseudo-unitarity condition $|1 - T| - \sqrt{R_R R_L} = 0$ is shown in red, whereas the blue curve displays a measure for $\mathcal{PT}$-symmetry; when $[R_L + R_R]/2 - T < 1$ $\mathcal{PT}$-symmetry holds; $[R_L + R_R]/2 - T = 1$ is the spontaneous symmetry breaking (SSB) point and beyond that point for $[R_L + R_R]/2 - T > 1$ $\mathcal{PT}$-broken phase onsets. The black dashed line displays the SSB point, that separates the $\mathcal{PT}$-symmetric (blue) and $\mathcal{PT}$-broken (yellow) phases.

configurations in detail.

The most general solution for the Schrödinger's equation in regions with (ii,iii) and without (i,iv) the $\mathcal{PT}$-symmetric complex potential $V = V_R + iV_I$ in Fig. 1 are given by: $\psi(z) = Ae^{ik_0 z} + Be^{-ik_0 z}$ for $V = 0$ and $\psi(z) = Ce^{ik_1 z} + De^{-ik_1 z}$, for $V \neq 0$, where $k_0 = [2mE/\hbar^2]^{1/2}$, $k_1 = [2m(E - V)/\hbar^2]^{1/2}$, in which m is the mass of the spin-$\frac{1}{2}$ particle, E denotes the energy and A, B, C and D are to be determined by boundary conditions. For the four different regions given in Fig. 1 we can write the wavefunctions of the spin-$\frac{1}{2}$ particles and then use the appropriate boundary conditions to find reflection coefficients (from left and right) r_L, r_R and the transmission coefficient t, which in return gives right reflectance $R_R = |r_R|^2$ left reflectance, $R_L = |r_L|^2$ and transmittance $T = |t|^2$, which obey the pseudo-unitarity or in other words the generalized unitarity relation [13]:

$$|1 - T| = \sqrt{R_R R_L}. \tag{1}$$

After applying the boundary conditions, we obtain $r_L = N_L/D_L$ and $t_R = N_T/D_T$ where,

$$
\begin{aligned}
N_L &= [i\,\Omega_1 sin\Lambda + \Omega_0^* cos\Lambda][cos\Lambda^* - i\,\Omega_0^* sin\Lambda^*] \\
&\quad + [i\,sin\Lambda^* - \Omega_0^* cos\Lambda^*][cos\Lambda + i\,\Omega_0 sin\Lambda], \\
D_L &= [cos\Lambda - i\,\Omega_0 sin\Lambda][\Omega_0^* cos\Lambda^* - i\,sin\Lambda^*] \\
&\quad + [\Omega_0^* cos\Lambda - i\,\Omega_1 sin\Lambda][cos\Lambda^* - i\,\Omega_0^* sin\Lambda^*], \\
N_T &= [cos\Lambda - i\,\Omega_0 sin\Lambda] r_L + cos\Lambda + i\,\Omega_0 sin\Lambda, \\
D_T &= cos\Lambda^* - i\,\Omega_0^* sin\Lambda^*.
\end{aligned} \tag{2}
$$

Here, $\Lambda \equiv k_1 L/2$, $\Omega_0 \equiv k_0/k_1$, $\Omega_1 \equiv k_1/k_1^*$. From those, r_R and t_L can be found by exploiting the symmetry: when $k_1 \mapsto k_1^*$, then $r_L \mapsto r_R$ and $t_R \mapsto t_L$. Moreover, due to reciprocity in transmission, $t_L = t_R$, so we can drop the left/right subscript, and write it as t. Fig. 2(a) show R_L, R_R, and T for varying E. Analogous to the $\mathcal{PT}$-symmetric optics, ATRs, where either $T = 1$, $R_L = 0$ or $T = 1$, $R_R = 0$ [13] are also achievable in our system and can be seen in Fig. 2(a). An important result displayed in Fig. 2(a) is that it is possible to obtain both consecutive ATRs from left/right by fine-tuning the energy as well as separated regions of left/right ATRs, still accessible via varying the energy, which is advantageous for device applications. The validity of pseudo-unitarity condition $|1-T| - \sqrt{R_R R_L} = 0$ is displayed in Fig. 2(b). Another important feature shown in Fig. 2(b) is a measure for the spontaneous symmetry breaking (SSB) point where the $\mathcal{PT}$-breaking transition onsets. The measure is given in terms of reflectances and transmittance where the SSB point is given by $[R_L + R_R]/2 - T = 1$; separating the $\mathcal{PT}$-symmetric ($[R_L + R_R]/2 - T < 1$) and $\mathcal{PT}$-broken ($[R_L + R_R]/2 - T > 1$) phases [13].

III. $\mathbb{S}$-MATRIX CALCULATIONS

The transfer matrix $\mathbb{M}$ and the scattering matrix $\mathbb{S}$ for our system are defined as: $\vec{\psi}^{(R)}(z) = \mathbb{M}\vec{\psi}^{(L)}(z)$ and $\vec{\psi}_o(z) = \mathbb{S}\vec{\psi}_i(z)$ with,

$$
\begin{aligned}
\vec{\psi}^{R,L}(z) &= [\psi_{i,\uparrow}^{R,L}(z), \psi_{o,\uparrow}^{R,L}(z), \psi_{i,\downarrow}^{R,L}(z), \psi_{o,\downarrow}^{R,L}(z)]^T, \\
\vec{\psi}_{i,o}(z) &= [\psi_{i,o,\uparrow}^{L}(z), \psi_{i,o,\uparrow}^{R}(z), \psi_{i,o,\downarrow}^{L}(z), \psi_{i,o,\downarrow}^{R}(z)]^T.
\end{aligned} \tag{3}
$$

All 16 possible combinations of L_i, R_i, and M where $i = 0, 1, 2$ yields three different eigenvalue spectra. The $\mathbb{S}$-matrices for different combinations yielding the same eigenvalue spectra are connected by unitary transformations thus do not display new physics, so it is sufficient to consider these three cases. Let us first describe how the SFs affect the structure of the $\mathbb{S}$-matrices. When no SFs are inserted, the two-by-two diagonal blocks for each spin in the $\mathbb{S}$-matrix are uncoupled. Mathematically, the effect of SFs is to mix the definite spin parts of the $\mathbb{S}$-matrices. To give a full recipe for t: if there are even number of any of the F_0 and F_1 components and/or any number of F_2 components inserted, position of t is unchanged, whereas if there are odd number of any of the F_0 and F_1 components and any number of F_2 components inserted, position of t is shifted to the opposite spin entry in the $\mathbb{S}$-matrix; for r_R/r_L, if there is an R_1/L_1 component inserted, position of r_R/r_L is unchanged, on the other hand if an R_0/L_0 or R_2/L_2 component is inserted, position of r_R/r_L is shifted to the opposite spin entry in the $\mathbb{S}$-matrix. The effect of SFs on the $\mathbb{S}$-matrices can be fully understood by investigating Fig. 1(c) and Table I. We will go over these effects below for the nontrivial cases, case 2 and case 3.

Going back to the three cases, the first one (case 1) is the most trivial case where the spin degrees of freedom are uncoupled due to the absence of SFs.

$$
\mathbb{S}^{(1)} = \begin{pmatrix} r_R & t & 0 & 0 \\ t & r_L & 0 & 0 \\ 0 & 0 & r_R & t \\ 0 & 0 & t & r_L \end{pmatrix}. \tag{4}
$$

yielding the same eigenvalues twice since spin degrees of freedom are uncoupled:

$$
\lambda_{1,2}^{(1)} = \frac{1}{2}\Big\{(r_R + r_L) \pm \sqrt{(r_R - r_L)^2 + 4t^2}\Big\}. \tag{5}
$$

Second case (case 2) displays coupling of spin degrees of freedom, yet no mixed state can be achieved. As an example, case 2 is obtained when $L_0 M R_0$ configuration is used, where M denotes the spin-independent $\mathcal{PT}$-symmetric potential component. Using the recipe described above, even number of F_0 components leave the placement of t unchanged in the $\mathbb{S}$-matrix and placement of R_0/L_0 components shifts the r_R/r_L entry to the opposite spin in the $\mathbb{S}$-matrix.

$$
\mathbb{S}^{(2)} = \begin{pmatrix} 0 & t & r_R & 0 \\ t & 0 & 0 & r_L \\ r_R & 0 & 0 & t \\ 0 & r_L & t & 0 \end{pmatrix}. \tag{6}
$$

Four eigenvalues for this configuration are given as:

$$
\lambda_{1-4}^{(2)} = \frac{1}{2}\Big\{ \pm (r_R + r_L) \pm \sqrt{(r_R - r_L)^2 + 4t^2}\Big\}. \tag{7}
$$

The last case (case 3) is the most interesting case where the mixed state of eigenvalues, i.e. coexistence of $\mathcal{PT}$-symmetric and $\mathcal{PT}$-broken eigenvalues is realized. Let us investigate the configuration $L_0 M$ as an example for this case. Since we have odd number of F_0 components, t is shifted to the opposite spin entry in the $\mathbb{S}$-matrix and also that component being L_0, r_L is also shifted to the opposite spin entry in the $\mathbb{S}$-matrix.

$$
\mathbb{S}^{(3)} = \begin{pmatrix} r_R & 0 & 0 & t \\ 0 & 0 & t & r_L \\ 0 & t & r_R & 0 \\ t & r_L & 0 & 0 \end{pmatrix}. \tag{8}
$$

This configuration yields the following eigenvalues:

$$
\lambda_{1,2}^{(3)} = \frac{1}{2}\Big\{(r_R + r_L) \pm \sqrt{(r_R - r_L)^2 + 4t^2}\Big\}, \tag{9a}
$$

$$
\lambda_{3,4}^{(3)} = \frac{1}{2}\Big\{(r_R - r_L) \pm \sqrt{(r_R + r_L)^2 + 4t^2}\Big\}. \tag{9b}
$$

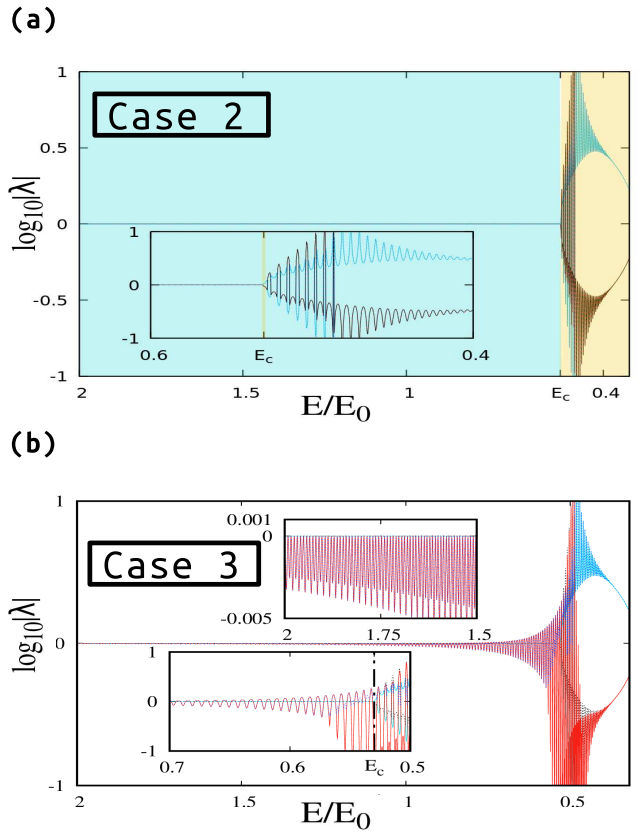


FIG. 3. **(a)** The magnitudes of the eigenvalues of $\mathbb{S}^{(2)}$, corresponding to case 2, versus the dimensionless energy scaled with $E_0 = 1\ eV$ are shown in log_{10} scale for $V_R/E_0 = 0.3$, $V_I/E_0 = 0.005$. The eigenvalues of $\mathbb{S}^{(2)}$ do not display phase mixing and the $\mathcal{PT}$-symmetric (blue) and $\mathcal{PT}$-broken (yellow) eigenvalues exist in separate E values. **(b)** For case 3, the first set of eigenvalues $\lambda^{(3)}_{1,2}$ which are $\mathcal{PT}$-symmetric before the SSB point are displayed in teal and black, whereas the second set, $\lambda^{(3)}_{3,4}$ displayed in red and blue, which are $\mathcal{PT}$-broken even far before hitting the SSB point, as shown in two insets.

The eigenvalues of the $\mathbb{S}$-matrices are unimodular for the $\mathcal{PT}$-symmetric phase. When $\mathcal{PT}$-symmetry is broken, they become reciprocal pairs.

IV. RESULTS

Fig. 3 displays the $\mathcal{PT}$-symmetric and $\mathcal{PT}$-broken eigenvalues for a structure with realistic parameters of $L = 0.5$ microns, $V_R/E_0 = 0.3$ and $V_I/E_0 = 0.005$ with varying energy spectra (scaled with $E_0 = 1\ eV$) for case 2 and case 3. As mentioned hereinabove, for the eigenvalues of $\mathbb{S}^{(2)}$, i.e. case 2, no phase mixing can be obtained for any E, as shown in Fig. 3(a). For case 3, the two different sets of eigenvalues corresponding to $\mathbb{S}^{(3)}$ have a different behavior as shown in Fig. 3(b): The first set of

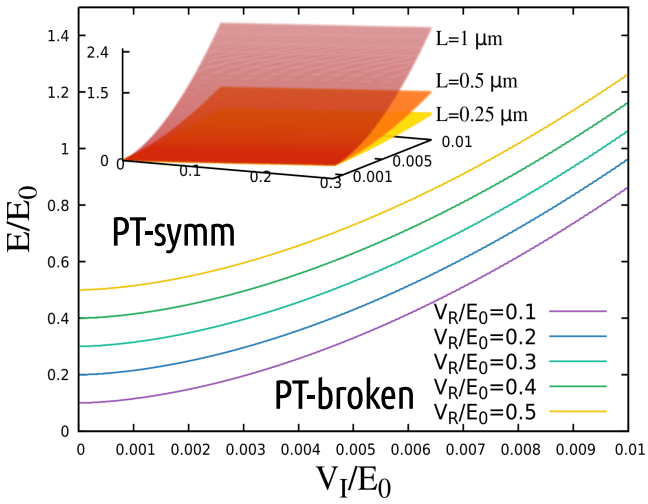


FIG. 4. The curves for the case $L = 0.5$ microns separating the $\mathcal{PT}$-symmetric upper and $\mathcal{PT}$-broken lower parts for varying V_R/E_0 values and the manifold (inset) of SSB, which separates the $\mathcal{PT}$-symmetric upper and $\mathcal{PT}$-broken lower parts for the given set of variables for $L = 0.25$ (yellow), 0.5 (orange) and 1 microns (red) are shown.

TABLE I. Different configurations depicted in Fig. 1(c).

configuration	eigenvalues	components	phase-mix	case
M	2	1	✗	1
L_0MR_0	4	3	✗	2
L_0M or **MR_0**	4	2	✓	3
L_1MR_1	4	3	✗	2
L_2MR_2	4	3	✗	2
L_1M or **MR_1**	4	2	✗	2
L_2M or **MR_2**	4	2	✓	3
L_0MR_1 or **L_1MR_0**	4	3	✓	3
L_0MR_2 or **L_2MR_0**	4	3	✗	2
L_1MR_2 or **L_2MR_1**	4	3	✓	3

eigenvalues $\lambda^{(3)}_{1,2}$ are $\mathcal{PT}$-symmetric before reaching the spontaneous symmetry breaking (SSB) point or in other words the critical energy $E_c \simeq 0.53$. Those eigenvalues are displayed in teal and black. The other set $\lambda^{(3)}_{3,4}$ are $\mathcal{PT}$-broken even far before reaching the SSB point. It is important to note that the magnitudes of $\lambda^{(3)}_{1,2}$ and $\lambda^{(2)}_{1-4}$ are equal, pointing that $\lambda^{(3)}_{3,4}$ are causing the mixing of $\mathcal{PT}$-symmetric and $\mathcal{PT}$-broken eigenvalues. The second set $\lambda^{(3)}_{3,4}$ are displayed in red and blue and the magnitudes of all four eigenvalues are plotted in log_{10} scale. Two insets of Fig. 3(b) display that even for large values of E/E_0 before reaching E_c, the second set $\lambda^{(3)}_{3,4}$ are $\mathcal{PT}$-broken, hence a broadband energy spectrum for phase mixing can be achieved.

Another significant result of this letter is displayed in Fig. 4, in which the curves for the case $L = 0.5$ microns separating the $\mathcal{PT}$-symmetric upper and $\mathcal{PT}$-broken lower parts for six different V_R/E_0 values are

shown. In the inset, the SSB manifold (with V_R dependence now explicitly shown together with V_I) is plotted for $L = 0.25, 0.5, 1$ microns with yellow orange and red, respectively, where L is the size of the component M. In the figure (and inset), the upper part of the curves (manifolds) corresponds to the set of variables that display $\mathcal{PT}$-symmetric eigenvalues for the $\mathbb{S}$-matrix and vice versa for the lower part.

Table. I summarizes all possible 16 configurations. The minimum number of components to achieve mixing is two. It is possible to achieve phase mixing also with three components. More interestingly, the configurations L_1M and MR_1 give no phase mixing, signifying the importance of the reflectance properties of the SFs over the transmittance properties for obtaining phase mixing.

Finally, as we demonstrated in the previous section, ATRs with extended features are accessible in our system. Fig. 2(a) displays that, consecutive ATRs from left/right by fine-tuning the energy as well as separated regions of left/right ATRs are accessible.

V. DISCUSSION AND CONCLUSIONS

The theoretical scheme that we proposed is promising for a variety of applications: The first one is in the field of spintronics. Similar to the applications of $\mathcal{PT}$-symmetry in optics, uni-directional invisibility, lasing, and other enthusing phenomena can be achieved in quantum mechanical systems. By introducing spin-$\frac{1}{2}$ particles and suggesting a structure that allows phase mixing demonstrated in this letter, it would be possible to achieve all of these properties selectively in spintronics based devices. Moreover, in our theoretical studies, we obtained switching between left/right ATRs both in a close neighborhood of energy values as well as in a relatively separated energy region, for the same parameter space, which is promising for non-reciprocal applications. The incoming energy of the fermionic species depend on their chemical potential which can be controlled through an applied gate potential, hence creating a controllable diode-like device. Secondly, in semiconductor-based devices, such as coupled quantum wells, obtaining mixed phase as suggested in this work would allow multi-functionality within a broadband spectrum. Lastly, the geometry in Fig. 1 can be extended to study a spin-dependent $\mathcal{PT}$-symmetric potential. This can be relevant in $\mathcal{PT}$-symmetric topological surface states with a strong spin-orbit coupling that has gained attention recently [36]. It is important to state that all of the parameters that we used in this letter have realistic values for the above-mentioned applications.

To conclude, we have theoretically demonstrated the mixing of $\mathcal{PT}$-symmetric and $\mathcal{PT}$-broken eigenvalues of the $\mathbb{S}$-matrix describing the one-dimensional spin-$\frac{1}{2}$ scattering problem from a spin-independent complex $\mathcal{PT}$-symmetric potential, for broadband energy spectra. We studied 16 different configurations obtained by combining SFs and M in all possible ways and categorized these in terms of their phase-mixing properties. Moreover, we discussed the analogies with $\mathcal{PT}$-symmetric optics and theoretically demonstrated the existence of ATRs with extended features in our scheme. We believe that our results will be promising for spintronics applications, semiconductor-based devices, and can contribute to the further understanding of topological surface states.

ACKNOWLEDGMENTS

One of the authors (E.O.) acknowledges partial support from the Turkish Academy of Sciences. This manuscript is originally published in EPL as *Europhys. Lett. 131 11001 (2020).*

[1] C. M. Bender and S. Boettcher, Phys. Rev. Lett. **80**, 5243 (1998).
[2] C. M. Bender, S. Boettcher, and P. N. Meisinger, J. Math. Phys. **40**, 2201 (1999).
[3] C. M. Bender, Rep. Prog. Phys. **70**, 947 (2007).
[4] A. Mostafazadeh, J. Math. Phys. **43** 205 (2002); *ibid.* **43** 2814 (2002); *ibid.* **43** 3944 (2002).
[5] R. El-Ganainy, K. G. Makris, D. N. Christodoulides, and Z. H. Musslimani, Opt. Lett. **32**, 2632 (2007).
[6] Z. H. Musslimani, K. G. Makris, R. El-Ganainy, and D. N. Christodoulides, Phys. Rev. Lett. **100**, 030402 (2008); J. Phys. A **41**, 244019 (2008).
[7] K. G. Makris, R. El-Ganainy, D. N. Christodoulides, and Z. H. Musslimani, Phys. Rev. Lett. **100**, 103904 (2008).
[8] S. Klaiman, U. Günther, and N. Moiseyev, Phys. Rev. Lett. **101**, 080402 (2008).
[9] A. Guo, G. J. Salamo, D. Duchesne, R. Morandotti, M. Volatier-Ravat, V. Aimez, G. A. Siviloglou, and D. N. Christodoulides, Phys. Rev. Lett. **103**, 093902 (2009).
[10] K. G. Makris, R. El-Ganainy, D. N. Christodoulides, and Z. H. Musslimani, Phys. Rev. A **81,** 063807 (2010).
[11] C. E. Rüter, K. G. Makris, R. El-Ganainy, D. N. Christodoulides, M. Segev, and D. Kip, Nature Phys. **6**, 192 (2010).
[12] H. Ramezani, T. Kottos, R. El-Ganainy, and D. N. Christodoulides, Phys. Rev. A **82**, 043803 (2010).
[13] L. Ge, Y. D. Chong, and A. D. Stone, Phys. Rev. A **85**, 023802 (2012)
[14] Z. Ahmed, Phys. Lett. A **377** 957 (2013).
[15] A. Mostafazadeh, J. Phys. A **47**, 505303 (2014).
[16] Z. Zhang, Y. Zhang, J. Sheng, L. Yang, M.-A. Miri, D. N. Christodoulides, B. He, Y. Zhang, and M. Xiao, Phys. Rev. Lett. **117** 123601 (2016).
[17] Y. Wu1, W. Liu, J. Geng, X. Song, X. Ye, C.-K. Duan, X. Rong, J. Du, Science **364** 878 (2019).
[18] X. Tan, Y. Zhao, Q. Liu, G. Xue, H. Yu, Z. D. Wang and Y. Yu, npj Quantum Mater. **2** 60 (2017).

[19] M. Chitsazi, H. Li, F. M. Ellis, and T. Kottos, Phys. Rev. Lett. **119** 093901 (2017).

[20] P. Peng, W. Cao, C. Shen, W. Qu, J. Wen, L. Jiang and Y. Xiao, Nat. Phys. **12** 1139 (2016).

[21] L. Feng, Z. J. Wong, R.-M. Ma, Y. Wang, X. Zhang, Science **346** 972 (2014).

[22] X. Zhu, L. Feng, P. Zhang, X. Yin, and X. Zhang, Opt. Lett. **38** 2821 (2013).

[23] D. L. Sounas, R. Fleury, and A. Alù, Phys. Rev. Appl. **4** 014005 (2015).

[24] Z. Lin, H. Ramezani, T. Eichelkraut, T. Kottos, H. Cao, and D. N. Christodoulides, Phys. Rev. Lett. **106** 213901 (2011).

[25] H. Cartarius and G. Wunner, Phys. Rev. A. **86** 013612 (2012); M. Kreibich, J. Main, H. Cartarius, and G. Wunner, Phys. Rev. A. **87** 051601(R) (2013).

[26] C. Hang, G. Huang, and V. V. Konotop, Phys. Rev. Lett. **110** 083604 (2013).

[27] C. M. Bender, Contemp. Phys. **46** 277 (2005).

[28] C. M. Bender Rep. Prog. Phys. **70** 947 (2007).

[29] R. El-Ganainy, K. G. Makris, M. Khajavikhan, Z. H. Musslimani, S. Rotter and D. N. Christodoulides, Nat. Phys. **14** 11 (2018).

[30] D. Christodoulides, J. Yang (Ed.), Parity-time Symmetry and Its Applications (Springer Nature Singapore 2018).

[31] C. M. Bender, PT-Symmetry in Quantum and Classical Physics (World Scientific, London, 2019)

[32] E. Özgün, A. E. Serebryannikov, E. Ozbay, and C. M. Soukoulis, Sci. Rep. **7** 15504 (2017).

[33] M. Khodas , A. Shekhter and A.M. Finkelstein Phys. Rev. Lett. **92** 086602 (2004).

[34] T. Hakioğlu, J. Phys.: Condens. Matter. **21** 026016 (2009).

[35] M. Razeghi, Fundamentals of Solid State Engineering, 3rd Edition (Springer USA 2009); M. Stepanova, S. Dew (Ed.), Nanofabrication Techniques and Principles (Springer Wien 2012).

[36] Y. X. Zhao, A. P. Schnyder, and Z. D. Wang, Phys. Rev. Lett. **116**, 156402 (2016); W. B. Rui, M. M. Hirschmann, and A. P. Schnyder, Phys. Rev. B **100**, 245116 (2019); C. Yuce and Z. Oztas, Sci. Rep. **8** 17416 (2018).